Master's Thesis

Medical Informatics Master

Universität Heidelberg / Hochschule Heilbronn

in Cooperation with Taipei Medical University

Predicting Blood Pressure from Photoplethysmogram Waveform Data: A Signal Processing and Machine Learning Approach

Supervisor:	Prof. Dr. Rolf Bendl
Co-Supervisor:	Prof. Dr. Syed Abdul Shabbir
Submitted by:	Hugas Jasinskas
Matriculation number:	202509
Submitted on:	February 18, 2024

Affidavit

I hereby declare under oath that I have independently prepared the present work without using sources other than those indicated; any thoughts taken directly or indirectly from external sources (including electronic sources) are identified as such.

The work has not been submitted to any examination authority, either domestic or foreign, in the same or similar form, and has not been published.

_____
Place, Date

_____
Signature

Contents

1 Abstract

2 Introduction

2.1 Subject and Motivation

Cardiovascular diseases (CVDs) are the leading cause of death worldwide, according to WHO publishing statistics [1]. One of the main factors contributing to CVDs is Hypertension. It is the leading risk factor for mortality, and is ranked third as a cause of disability-adjusted life-years [2]. Currently, there is a significant need for continuous blood pressure (BP) monitoring due to various factors. Primarily, while hypertension is a manageable condition, the availability of accurate high BP detection remains scarce, especially in low-resource environments [3]. Additionally, blood pressure (BP) is subject to rapid fluctuations influenced by various factors, including stress, emotions, dietary intake, physical activity, and medication usage [4]. Continuous monitoring of blood pressure, rather than relying on isolated measurements, plays a vital role in the early detection and treatment of hypertension [5].

The current accurate methods for measuring BP continuously are either invasive or involving a cuff-mechanism. Catheterization is internationally recognized as the "gold standard" for obtaining the most accurate measurement of continuous blood pressure [6]. However, due to its invasive nature and limited applicability to hospital settings, this method requires medical intervention, which renders it inconvenient for everyday use.

While cuff-based devices are commonly utilized for this objective, it is worth noting that around 30% of home blood pressure monitors are found to be inaccurate, rendering continuous measurement unfeasible [7, 8]. Moreover, this approach relies on the individual consciously and intentionally engaging in manual blood pressure monitoring, which poses limitations and might be often overlooked.

An ideal technology for measuring blood pressure should have the following attributes: non-invasiveness, cuffless operation, optical functionality, wearable design, and cost-effectiveness [5]. One approach satisfying these requirements is the estimation of BP from a single measurement PPG sensor. This approach, using two modes, reflectance and transmission, has gained an increasing amount of attention in the literature due its simplicity, and ability to provide continuous and cuffless measurement [5]. Typically, the photoplethysmography (PPG) technique has been traditionally employed in healthcare settings to measure heart rate [9] and blood oxygen saturation using a pulse oximeter [10].

Nevertheless, establishing a straightforward, distinct, and continuous relationship be-

tween these characteristics and blood pressure (BP) has proven to be challenging. To address this, the approach heavily depends on signal pre-processing techniques, extracting PPG features, and utilizing machine learning (ML) algorithms to estimate BP based on these features [5]. A recent scoping review by Knight et al. concluded that PPG can be successfully used to continuously measure BP, by evaluating latest publications and finding over 80% accuracy in detecting hypertension [11].

This study examines the current methods and aims to develop efficient approaches for the continuous and accurate measurement of blood pressure using PPG and addresses the following research questions:

1. **What is the relationship between PPG data and blood pressure among Intensive Care Unit (ICU) patients?**

2. **Can PPG-based data be used to estimate blood pressure accurately?**

2.2 Tasks and Objectives

The tasks of the thesis are as follows:

1. Signal Processing: to find an optimal data fetching and filtering approach from available MIMIC Databases.

2. Likewise, to create a consistent algorithm for key feature extraction.

3. Machine Learning: to develop a model based on the resulting features from Signal Processing, to reliably predict BP from PPG.

2.3 Structure of the Thesis

This thesis is organized as follows:

In Chapter 3, the foundations of the used terms and prerequisites for the methods are explained. For example, in 3.1, the terms "Blood Pressure" (3.1.1) and "Photoplethysmography" (3.1.2) are discussed. Furthermore, the general structure of MIMIC databases is explained (3.1.3). In addition, the essential information about the Computing part of this research is provided (3.2).

In Chapter 4, the methodology is explained.

Chapter 5 presents the results.

The focus of Chapters 6 and 7 is on summarizing the work. Here, both the future prospects for this research field and the next steps in relation to broader scope projects are presented.

3 Theoretical Background

3.1 Medical Background

3.1.1 Blood Pressure

Blood pressure (BP) is a physiological measure of the force exerted by circulating blood against the walls of the arteries [12]. It is highly dependent on blood flow, which refers to the movement of blood through a vessel, tissue, or organ. Blood circulation begins with the contraction of the heart's ventricles. This action generates a type of hydrostatic pressure, which is the force exerted by a fluid due to gravitational pull, typically against the walls of the container that confines it.

BP is a type of hydrostatic pressure, representing the force exerted by blood on the walls of blood vessels or the heart's chambers. While it can be assessed in various body regions, the term "blood pressure" without specific qualifiers commonly refers to systemic arterial BP. This denotes the pressure of blood within the arteries of the systemic circulation. In clinical settings, this pressure is measured in millimeters of mercury (mmHg) and is typically acquired using the brachial artery in the arm [13].

Measuring BP is crucial for assessing cardiovascular health and identifying potential risks. It allows for the early detection of conditions like hypertension and hypotension, enabling timely interventions to prevent serious cardiovascular events [14]. BP serves as a key indicator of the risk for heart attacks, strokes, and heart failure, guiding preventive measures and treatment strategies [15].

Various Types of Measurement

One of the most common BP measurement methods is one using a sphygmomanometer (see manual 1 and automatic 2 devices), also known as non-invasive blood pressure (NIBP), is typically recorded as numeric values at specific time intervals. The process involves inflating the cuff to temporarily stop blood flow and then gradually releasing the pressure to detect the sounds associated with the flow of blood through the brachial artery. Manually, the measurement entails one individual conducting the procedure on another, typically involving a healthcare professional administering the

assessment to a patient. Conversely, automatic measurement allows the patient to independently measure their blood pressure without external assistance. Both approaches yield comparable measurements of the same nature. The two primary values obtained are systolic pressure (maximum pressure during heartbeats) and diastolic pressure (minimum pressure between heartbeats). During the process of cuff inflation and deflation, each heartbeat generates characteristic sounds (Korotkoff sounds) that are detected by a stethoscope placed over the brachial artery. Systolic pressure is recorded when the first tapping sounds are heard, and diastolic pressure is recorded when the sounds disappear or change character. This beat-to-beat approach provides information about individual fluctuations in blood pressure [13].

Figure 1: Standard Sphygmanometer [16]

Figure 2: Automatic Digital Sphygmanometer [17]

Although measuring blood pressure with a cuff using a sphygmomanometer is widely adopted as a common and convenient method, it is not without its constraints. Studies, such as those by Leung et al. and Sebo et al. , have highlighted the inability of home blood pressure monitoring devices to consistently and accurately detect hypertension [7, 8]. Furthermore, a significant limitation lies in its inability to provide continuous and consistent monitoring, necessitating patients to actively remember and engage in the effort to measure their blood pressure. This intermittent approach using a cuff provides

valuable insights into systolic and diastolic pressures at specific time intervals, but it may not capture the nuanced changes that occur between measurements. To address the need for continuous monitoring, other methods, such as arterial catheterization, are employed.

Arterial catheterization (illustrated in Figure 3) is commonly employed in critical patient care, serving dual purposes: continuous blood pressure monitoring and obtaining frequent blood gas measurements. Typically conducted at bedside, the procedure utilizes percutaneous methods like the Seldinger technique to cannulate arteries [18]. The resulting arterial blood pressure (ABP) is a dynamic parameter that can change with each heartbeat, and it is typically represented as a waveform rather than a single numeric value. The ABP waveform consists of two main components: systolic pressure and diastolic pressure. Such continuous monitoring of ABP is usually done in clinical settings, using an arterial line connected to a pressure transducer. The resulting waveform is displayed on a monitor in real-time. However, for ease of interpretation and documentation, numeric values are commonly extracted from the waveform at specific time intervals [19].
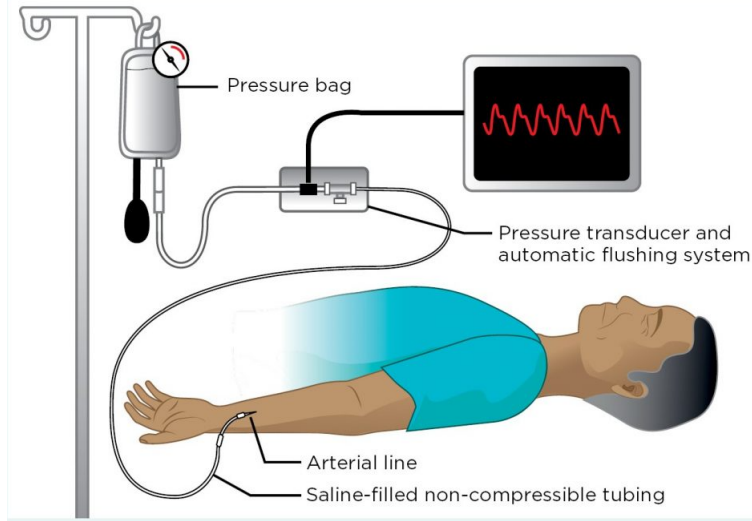

Figure 3: Arterial Catheterization and Stationary BP Monitoring [20]

In situations where high temporal resolution is crucial, ABP can be recorded beat-to-beat, providing a value for each heartbeat. This is particularly important in situations where rapid changes in blood pressure need to be closely monitored, such as during certain medical procedures or in critically ill patients [21].

For routine monitoring and documentation, numeric values are often averaged over a specific time interval, such as every 1, 5, or 15 minutes. This averaged value may

be reported as the mean arterial pressure (MAP), which is a weighted average of the systolic and diastolic pressures over a cardiac cycle [22] Some monitoring systems may also provide systolic and diastolic blood pressure readings at regular intervals.

Alternative approaches for measuring BP have emerged over the past years. Volume clamping [23] and tonometry [24] are some of the other methods. These non-invasive techniques offer continuous monitoring of blood pressure values. Volume clamping, which involves the use of a small finger cuff and a PPG sensor, is one method for continuous blood pressure measurement. Tonometry, on the other hand, is a cuffless approach that utilizes a manometer-tipped probe pressed directly on an artery. The volume clamping approach allows for instantaneous and prolonged blood pressure measurement. However, it is associated with high costs and still necessitates the use of a cuff, which can be inconvenient and uncomfortable. Conversely, the tonometry method is sensitive to movement of the arm and probe, making it challenging to maintain accuracy in practical applications. Additionally, constant calibration with a cuff blood pressure device is required [25].

In conclusion, blood pressure serves as a critical physiological measure, representing the force exerted by blood on the walls of blood vessels. The conventional method of measuring blood pressure with a cuff and sphygmomanometer provides valuable insights into systolic and diastolic pressures but is limited by its intermittent nature. To address the need for continuous monitoring, arterial catheterization is commonly employed in critical care, offering real-time data through a dynamic waveform. Alternative non-invasive approaches like volume clamping and tonometry aim to provide continuous blood pressure monitoring, but they come with their own challenges and considerations. As technology advances, these methods contribute to a comprehensive understanding of blood pressure dynamics, facilitating improved patient care and risk assessment.

3.1.2 Photoplethysmography

Photoplethysmography (PPG) is an optical measurement technique designed to identify changes in blood volume within the microvascular bed of tissue [26]. Its clinical application is extensive, as the technology is integrated into commercially available medical devices, including pulse oximeters, vascular diagnostics, and digital beat-to-beat blood pressure measurement systems. The fundamental structure of PPG technology is straightforward, requiring only a few opto-electronic components: a light source for tissue illumination, usually a light-emitting diode (LED) and a photodiode (PD) to gauge slight variations in light intensity correlated with changes in perfusion in the catchment

volume.

History

One of the first mentioned instances on the use of PPG were recorded in 1936 by Molitor and Kniazuk [27]. They outlined comparable devices employed for tracking alterations in blood volume in the rabbit ear under conditions of venous occlusion and the administration of vasoactive drugs. A pioneer who helped establish the PPG technique was Alrick Hertzman [28]. In his 1937 paper, Hertzman coined the term "Photoelectric Plethysmograph" etymologically meaning: photo - "light", plethora - "exess of body fluid, blood", graph - "something written". He detailed the application of a reflection mode system to assess alterations in blood volume within the fingers, particularly during the Valsalva maneuver [29], exercise, and exposure to cold. This contribution not only demonstrated the versatility of the technique but also underscored its potential clinical relevance.

Hertzman and Spealman [28] outlined two crucial features of the PPG pulse waveform. They categorized the pulse appearance into two phases: the anacrotic phase representing the ascending edge of the pulse, and the catacrotic phase representing the descending edge of the pulse. The initial phase primarily corresponds to systole, while the subsequent phase relates to diastole and wave reflections from the periphery. In individuals with healthy compliant arteries, a dicrotic notch is commonly observed during the catacrotic phase.

In the late 1970s, there arose a renewed interest in the PPG technology, driven by the demand for compact, dependable, cost-effective, and user-friendly noninvasive cardiovascular assessment techniques [30]. The progress in opto-electronics and clinical instrumentation has played a significant role in advancing PPG technology. Semiconductor advancements, particularly in LEDs, photodiodes, and phototransistors, have brought about substantial improvements in the size, sensitivity, reliability, and reproducibility of PPG probe design. A significant leap in the clinical application of PPG-based technology occurred with the introduction of the pulse oximeter [31]. This device revolutionized non-invasive monitoring of patients' arterial oxygen saturation, marking a major advancement in the field.

Other emerging technologies encompass PPG imaging technology, telemedicine, and remote monitoring. In 2005, Wieringa et al. detailed a contactless multiple-wavelength PPG imaging system designed primarily for remotely imaging the distribution of arterial oxygen saturation (SpO2) within tissue [32]. The system captures movies of two-dimensional matrix spatially resolved PPG signals at different wavelengths during res-

piratory changes. PPG was found to have substantial potential in telemedicine, particularly for remote/home health monitoring of patients. Miniaturization, user-friendliness, and robustness stand as pivotal design criteria for such systems. This is exemplified by finger ring-based PPG sensors for monitoring beat-to-beat pulsations ([33], [34]).

Most PPG devices these days either use the transmissive or reflective operating modes (illustrated in Figure 4). Currently, the prevalent method is the transmissive mode, chosen for its notable accuracy and stability [35]. However, there is a growing interest in reflective-mode PPG due to its elimination of the need for a thin measurement site. This method proves versatile, applicable to various sites such as the feet, forehead, chest, and wrists. Especially when the wrist serves as the designated measurement site, PPG sensors can be conveniently employed in the form of a band or watch.
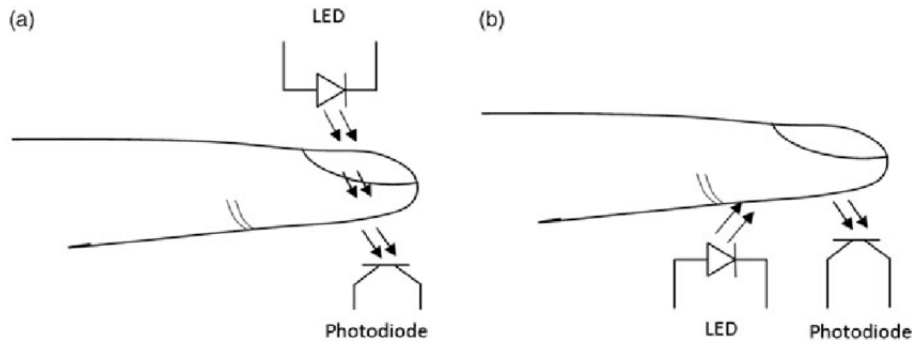
Figure 4: PPG Transmission (a) and Reflection (b) operating modes [36]

Working Principle

The PPG signal consists of pulsate (AC) and superimposed (DC) components (see Figure 5). The AC component originates from variations in blood volume associated with heartbeats, while the DC component is influenced by factors such as respiration, sympathetic nervous system activity, and temperature regulation [37]. The AC component specifically illustrates changes in blood volume during phasic cardiac activity, representing both the systolic and diastolic phases. The systolic phase, also known as the "rise time" initiates with a valley and concludes at the pulse wave systolic peak. The pulse wave concludes with another valley at the end of the diastolic phase [38]. In most PPG waveform analyses including this one, the AC component in the form of a waveform signal is used.

Use Cases

PPG finds diverse applications in clinical settings, covering physiological monitoring
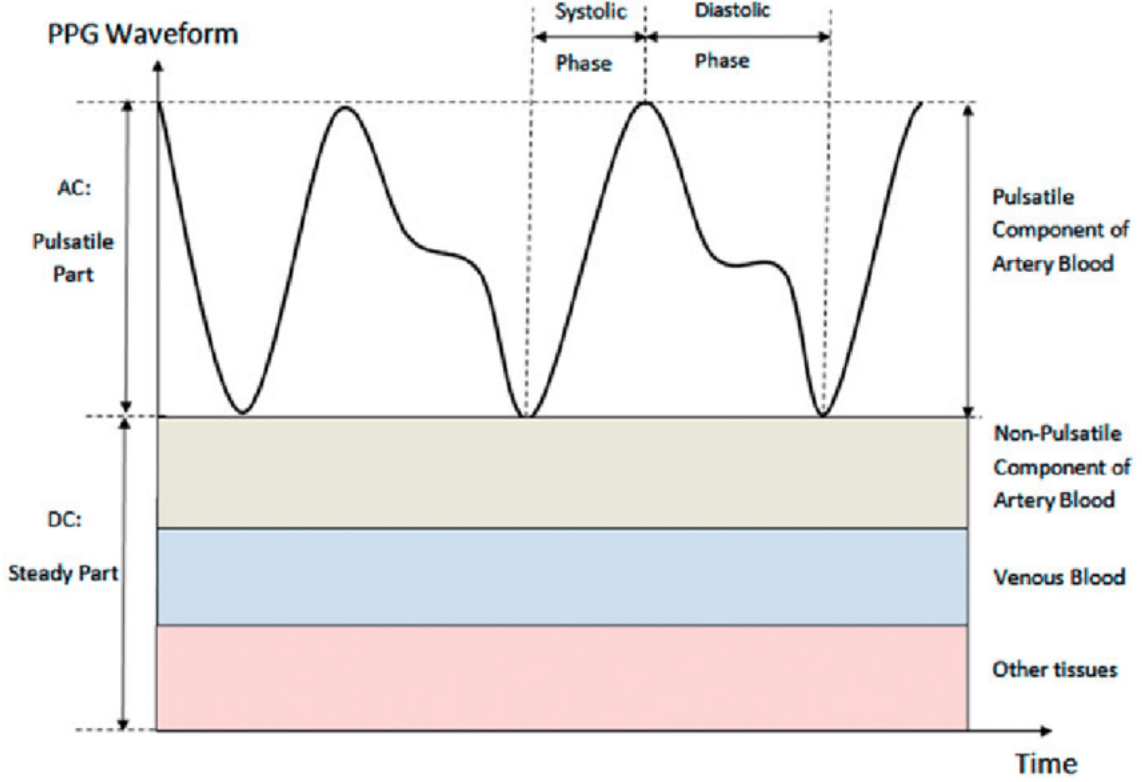
Figure 5: AC and DC components of the PPG signal [36]

(such as blood oxygen saturation and heart rate), vascular assessment (including arterial disease, aging and tissue viability), and autonomic function evaluations (such as thermoregulation, heart rate and other assessments of cardiovascular variability) [37]. Furthermore, the popularity of PPG technology as an alternative for monitoring heart rate has risen recently, primarily attributed to its ease of use, user-friendly wearing comfort, and cost-effectiveness [39]. Nowadays, almost every wearable devices uses the PPG technology to track the user's heart rate and other extractable vital parameters [40]. PPG sensors in mobile and wearable devices typically feature red, green, or both light-emitting diodes. Most devices incorporate a green-light PPG sensor for continuous heart rate monitoring during daily activities. Some devices also include red-light PPG sensors, which are effective for measuring heart rate when a person is stationary, providing insights into hydration, muscle saturation, and total hemoglobin. While red-light PPG can penetrate tissue layers more deeply using near-infrared spectroscopy, it is susceptible to disturbance from ambient light. In contrast, green light, being less absorbed by the skin, minimizes the impact of ambient light noise on the heart rate signal. As a result, wearable devices commonly utilize green light rather than red-light PPG [41]. Different

types of devices implement the PPG technology. It can be found in pulse oximeters, smartphones, smartwatches and other wearable devices (examples in Figure 6).

Figure 6: AC and DC components of the PPG signal [42]

In conclusion, the PPG is an optical sensor, consisting of an LED paired with a PD, hence it is simple, inexpensive and can be easily build into a wearable device. The PPG waveform can be obtained using two modes, reflectance and transmission. This waveform corresponds to the blood volume in blood vessels. Traditionally employed in healthcare for heart rate and blood oxygen saturation measurements, particularly with pulse oximeters, the PPG plays a pivotal role [37].

Additionally, peripheral volumetric changes exhibit correlation with BP [43]. Utilizing characteristic PPG features, ML functions can estimate Systolic BP (SBP) and Diastolic BP (DBP). However, establishing a simple, clear, and continuous relationship between these features and BP remains elusive. This method heavily relies on signal preprocessing, feature extraction, and the application of ML algorithms for BP estimation based on these features.

3.1.3 MIMIC Databases

Patient records and documentation are crucial for maintaining a comprehensive overview of medical history, aiding in accurate diagnosis, treatment planning, and ensuring conti-

nuity of care. They also serve as legal documents, providing evidence of the care provided and facilitating communication among healthcare professionals. Collecting digital data during routine clinical practice has become widespread across hospitals. Over time, a pattern has emerged in the collection and storage of patient data for subsequent utilization in future research endeavors.

Origin

In 1996, two researchers at the Massachusetts Institute of Technology, George B. Moody and Roger G. Mark, introduced the Multiparameter Intelligent Monitoring in Intensive Care (MIMIC) Database (DB). The DB was derived from patient monitors in the medical, surgical, and cardiac ICUs of Boston's Beth Israel Hospital [44]. The first instance of the DB included 100 patient records, each typically containing between 24 and 48 hours of continuous recorded data. The second version of the DB (MIMIC-II) was introduced in 2011 boasting a notably larger sample size and a wider scope of information sourced entirely from diverse digital information systems [45]. MIMIC-III [46] was finalized in 2016, marking a significant expansion from MIMIC-II, with data available from over 40,000 patients. The fourth and latest MIMIC DB was publicly released in 2023 spanning a decade of admissions from 2008 to 2019. MIMIC-IV was announced to enhance the realm of publicly accessible critical care datasets, by integrating precise digital sources like the electronic medicine administration record and featuring a modular structure enabling seamless integration with external departments and diverse data modalities [47]. The diagram in Figure 7 depicts the component interaction for data and information delivery to the publicly available DB.
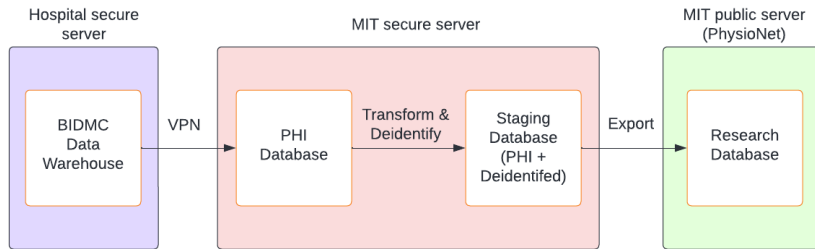

Figure 7: Workflow between Beth Israel Deaconess Medical Center (BIDMC), Protected Health Information (PHI) DB [48]

Structure

Both the MIMIC-III and MIMIC-IV DBs are cited and employed in this investigation, exhibiting comparable structures (depicted in Figure 8), encompassing diverse data cat-

egories. However, the primary emphasis of this inquiry lies in the Waveform Section of the DB (highlighted by a red rectangle in Figure 8). The waveform DB comprises individual records, each representing a patient's ICU stay and stored in a distinct subdirectory. These records lack specific date or time data to ensure patient anonymity, relying instead on elapsed time from the record's start. Supplemented by surrogate date and time information for cross-referencing with other DB modules. Waveforms denote regularly sampled, high-resolution measurements stored in a signal specific numerical format. To optimize storage and processing, these waveforms are segmented into intervals, maintaining continuous sampling within each segment despite potential signal unavailability throughout a patient's ICU stay.
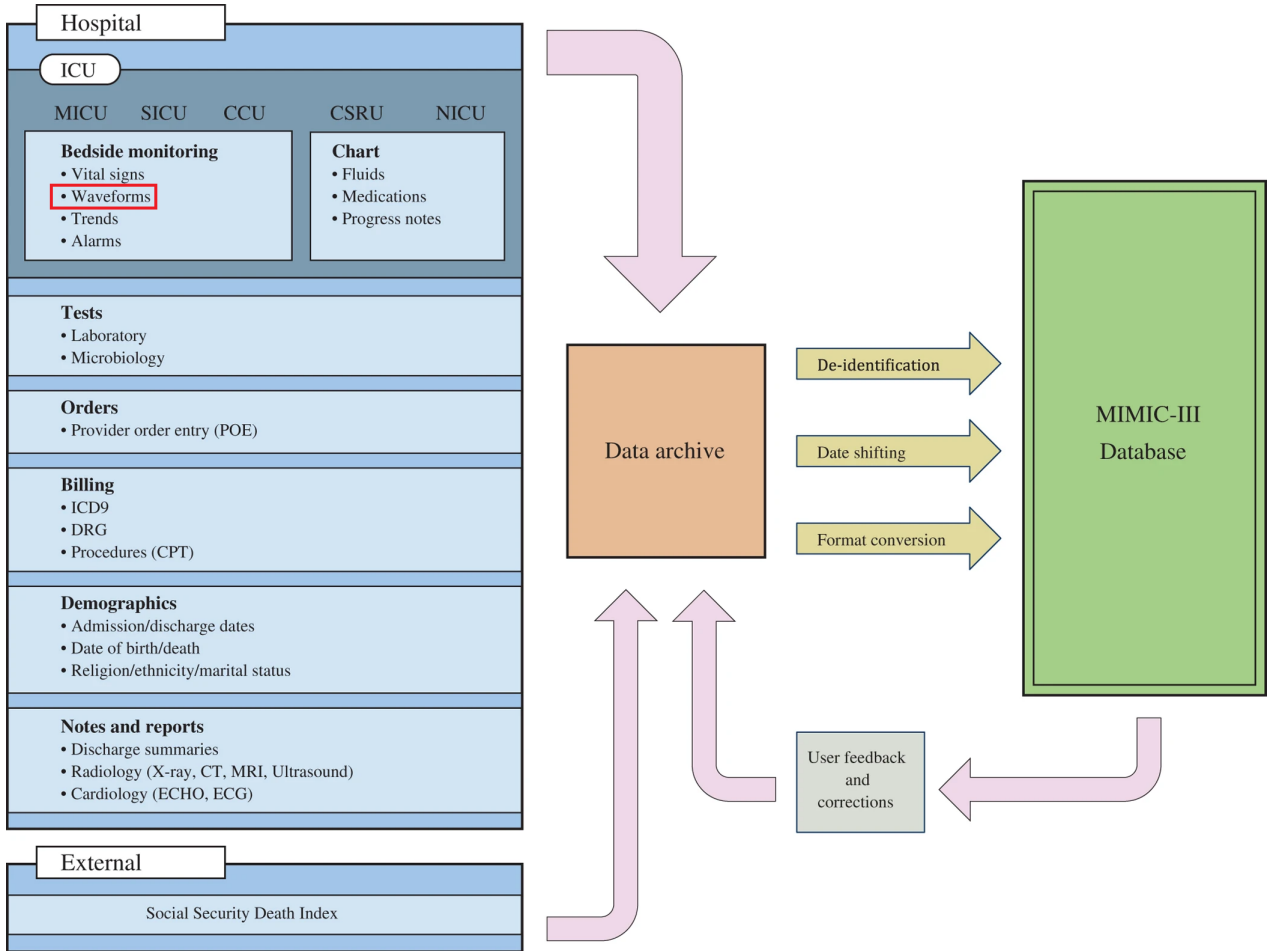

Figure 8: General Structure of the MIMIC-III DB [46]

The Waveform data from both the MIMIC-III and MIMIC-IV DBs is publicly available on the Physionet internet website [49, 50]. In both DBs recorded waveforms typically encompass one or more electrocardiogram(ECG) signals, often feature continuous ABP

15

waveforms and fingertip PPG signals. Numeric data typically includes heart and respiration rates, SpO2, and systolic, mean, and diastolic blood pressure, among other metrics when accessible. Recording durations also vary, with most lasting a few days, although some are shorter and other might even extend over several weeks. Both projects consist of two types of data: waveform data, comprising high-resolution, regularly sampled time series obtained directly from measuring devices, and numeric data, including digitally derived values or irregularly sampled data (like NIBP).

Differences and Similarities between MIMIC-III and MIMIC-IV

In MIMIC-III, waveforms were collected in a largely automated manner from selected adult and neonatal ICUs, resulting in a random sample of patients. The data archiving process was not continuous, and the recorded waveforms and numerics varied based on ICU staff choices. The individual patient consent waived due to de-identification. On the other hand, MIMIC-IV collected data from ICUs where bedside monitors were linked to a local area network, allowing continuous monitoring and data transfer to a proprietary relational DB. Data was stored for several weeks before being retrieved and archived daily. The de-identification process for MIMIC-IV followed the same method as MIMIC-III, removing or replacing protected health information with non-identifying information.

Both the MIMIC-III and MIMIC-IV DBs encompass waveform and numeric datasets sourced from ICUs. While both datasets feature detailed waveform records and numerical values, their storage and acquisition methods differ. MIMIC-III organizes its records within a directory structure with segmented waveform data, while MIMIC-IV adopts WFDB format for waveforms and compressed CSV files for numerics. However, MIMIC-IV incorporates enhancements like automated record partitioning and optimized storage formats to enhance data management efficiency.

Clinical Research DBs such as MIMIC play a pivotal role in facilitating global access to critical patient data, thereby supporting scientific endeavors across various medical domains. By ensuring the anonymity and de-identification of patient information, these DBs uphold stringent standards of data privacy and ethics, thereby avoiding any infringement upon patient rights or privacy regulations. Such DBs serve as invaluable resources for conducting comprehensive studies spanning diverse medical disciplines, including but not limited to the detection and treatment of various cancers, cardiovascular diseases, and even neonatal care in stationary settings. Their expansive datasets offer researchers an extensive pool of information to draw insights from, ultimately advancing

the overall understanding and management of complex medical conditions.

3.2 Computing Background

3.2.1 Signal Processing

This section explores various techniques and methods employed in the analysis of PPG signals and their correlation to BP measurements. PPG-based BP estimation has emerged as a promising non-invasive approach, utilizing waveform observations from signals like PPG signals from different anatomical sites or their combination with ECG signals. This section delves into the diverse methodologies and algorithms utilized for processing PPG signals to derive meaningful insights into BP dynamics.

PPG Signal Processing Methods

Previous research has documented an inverse relationship BP and pulse transit time (PTT) [51]. Extensive investigation over past decades has focused on the PTT-based approach, revealing growing support for its potential in offering non-invasive BP measurements without the need for cuffs. PTT refers to the delay in time for the pressure waveform to traverse between two arterial locations (see Figure 9). It can be calculated as the time difference between proximal and distal waveforms indicative of the arterial pulse.
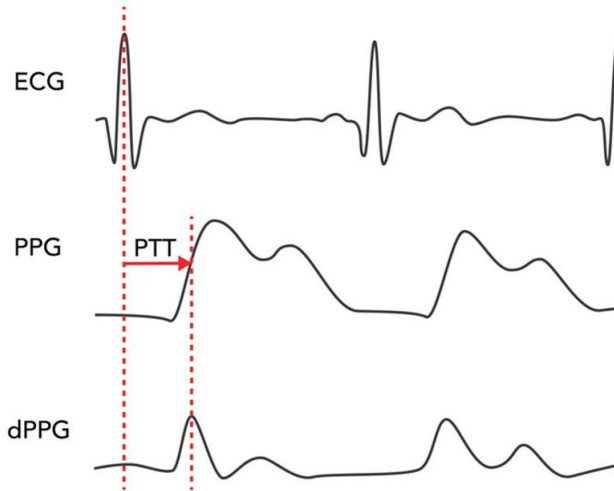

Figure 9: Calculation of PTT from ECG, PPG and first PPG derivative waveforms [52]

Pulse arrival time (PAT) represents another widely employed technique [6]. It is defined as the time that takes the pulse wave to travel from the heart to a peripheral

site e.g. finger, toe, etc. It denotes the temporal discrepancy between the R-peak of the ECG signal and the peak of the PPG signal, measured within the same cardiac cycle (see Figure 10). Both PTT and PAT require simultaneous measurement at two different sites on the body, hence two measurement sensors (ECG and PPG) are needed for recording the signals in order to estimate these parameters.
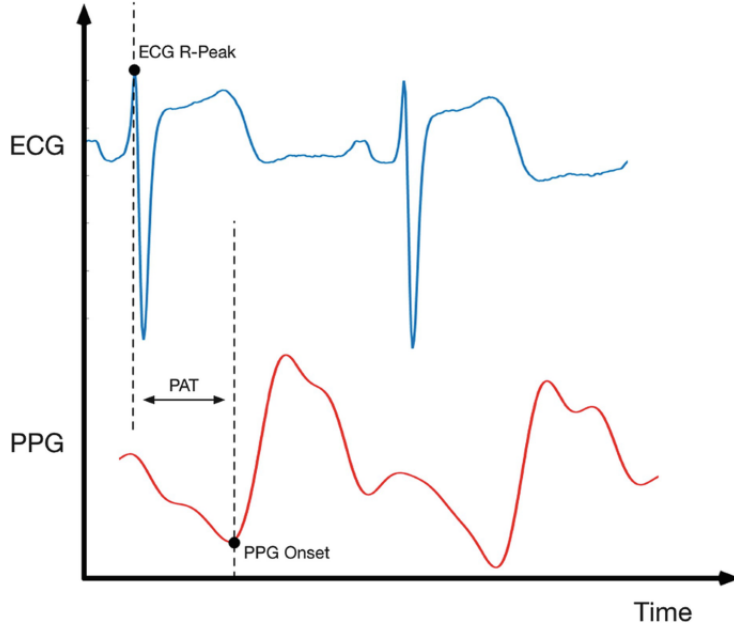

Figure 10: Calculation of PAT from ECG and PPG waveforms [53]

Pulse wave velocity (PWV) is another alternative method for estimating BP [54]. PWV determines the speed of the pulse wave by utilizing two PPG sensors positioned along the same arterial branch, separated by a known distance (see Figure 11), portrayed by the following formula $PWW = \frac{D}{PTT}$ where D is the distance between two known body parts.

Estimating BP through PTT, PAT, or PWV parameters involves mathematical models, but implementing these models faces challenges, and none of these techniques has become a reliable clinical tool for BP measurement. Challenges include the need for synchronized sensors, varying sampling rates, and reliance on complex arterial wave propagation models, making continuous BP measurement inconvenient and requiring constant calibration. Despite per-person calibration, these models offer only short-term BP estimation and remain unreliable for beat-to-beat BP measurement.

Pulse wave analysis (PWA) offers a multifaceted solution to the previously mentioned issues. It serves as an umbrella term encompassing signal processing and feature extraction of certain PPG waveform characteristics. PWA offers a novel method for cuffless,
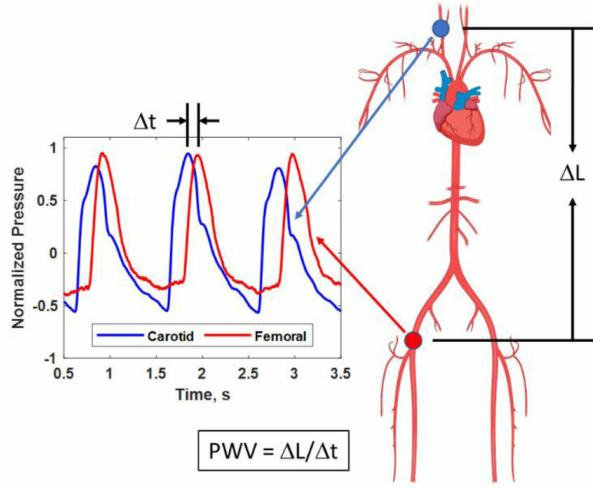
Figure 11: Calculation of PWW from two PPG signals at different body parts [55]

continuous, and calibration-free BP measurement by extracting temporal features from the PPG waveform, which demonstrate a strong correlation with individual BP levels [56]. Utilizing only one PPG sensor, PWA presents several advantages over previous methods, including simplicity, affordability, straightforward signal acquisition, and a resemblance between BP pulse waveform and PPG blood volume pulse (example in Figure 12). This data-driven approach to BP estimation provides optical BP measurement with promising potential for practical applications. Advancements in computational technology and data analysis software have simplified the preprocessing and analysis of physiological signals. Techniques such as filtering and feature extraction are commonly utilized in the analysis of PPG pulse waves, often integrated into ML and deep neural network (DNN) models for blood pressure estimation.
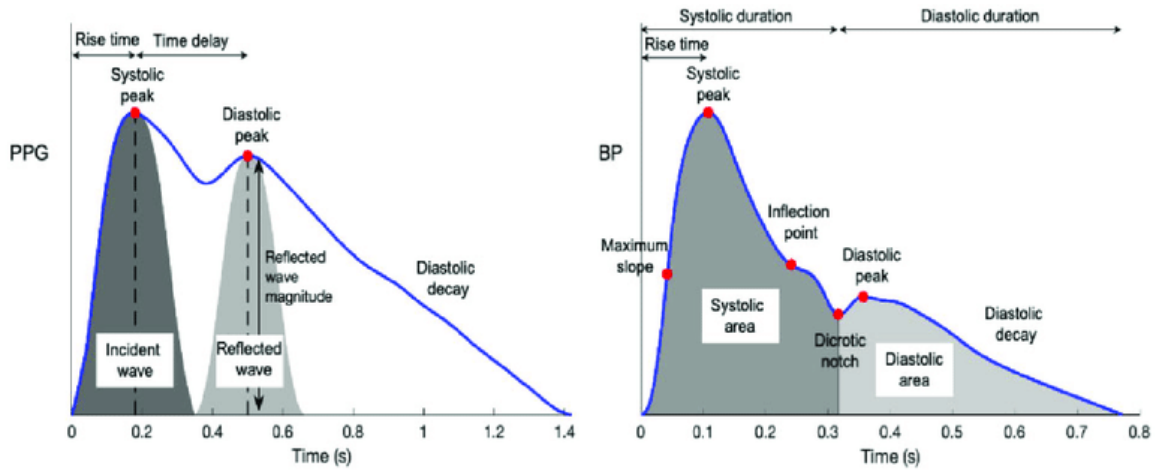

Figure 12: Example of a PWA used to extract features from the PPG waveform [57]

Signal Pre-Processing

The preprocessing of physiological signals, crucial for accurate BP estimation, involves a variety of signal filtering techniques. Techniques like Chebyshev, Butterworth, and Savitzky-Golay filtering, along with methods such as second derivative analysis, play pivotal roles in enhancing signal quality. These preprocessing steps, facilitated by advancements in computational technology, pave the way for more refined analysis and interpretation of PPG pulse waves.

An investigation into various signal pre-processing techniques necessitates an examination of different types of filters. One prominent representative is the Butterworth filter, characterized by its flat frequency response within the passband. Belonging to the Infinite Impulse Response (IIR) category, Butterworth filters offer efficiency in processing low-frequency signals and exhibit rapid computational capabilities, as demonstrated by Chatterjee et al. in their PPG-based heart rate analysis [58]. The filter order directly correlates with the number of energy storage components present in the analogous analog circuit, such as inductors and capacitors. The transfer function of a Butterworth filter is represented by the following formula, where n is the filter order and z is the complex variable used in Z-transform analysis:

$$H(z) = \frac{1}{[1+(z^{-1})^n]^{1/2}}$$

Another noteworthy filter type is the Savitzky-Golay filter, introduced by Savitzky and Golay [59]. Falling under the Finite Impulse Response (FIR) category, this filter effectively smooths data while removing unwanted frequencies. Its inherent stability ensures a finite output for any finite input. Additionally, the linear phase property guarantees the absence of frequency-dependent time shifts. The Savitzky-Golay filter doesn't have a single transfer function like the Butterworth filter because it belongs to the FIR category. Instead, it relies on convolution with pre-calculated coefficients specific to the desired characteristics. The filter fits a low-degree polynomial to a window of data points around each point in the signal. The smoothed value is then the value of the fitted polynomial at the center point. Different polynomial degrees and window sizes lead to different filtering effects. The relationship can be expressed by the following formula:

20

Furthermore, the Chebyshev filter offers a steeper roll-off compared to other filters, leading to sharper distinctions between desired and unwanted frequencies. While this advantage comes at the cost of controlled passband ripples, these filters remain valuable tools for applications requiring precise frequency separation. Beyond digital signal improvement, they find applications in audio crossovers, image noise reduction, and data communication, as discussed by Antoniou [60]. While the Chebyshev filter has a transfer function like the Butterworth filter, it's slightly more complex due to its specific characteristics. Unlike the Savitzky-Golay filter, its coefficients depend on the desired ripple level and order, making a single, universal formula impractical. The general form of the Chebyshev filter transfer function depends on whether it's Type I (equiripple in both passband and stopband) or Type II (equiripple only in the stopband). The corresponding functions are presented by the following formulas:

In their 2018 study, Liang et al. investigated nine different digital signal filters to identify the optimal approach for short PPG signals (2.1s) [61]. Some of the filters included the Butterworth, Elliptical, Chebyshev Type I and II, Median Filter etc. Their performance-based ranking revealed the Chebyshev II filter as the most effective in enhancing PPG signal quality, with the optimal order at 4th.

Miscellaneous Signal Processing Approaches

A study conducted by Takazawa et al. investigated the utilization of the second derivative of the fingertip PPG waveform within clinical contexts [62]. The research analysed changes in patients' pressure, wave ratios, age-related variations, and correlations with health conditions. Collectively, the results indicate the potential value of the second derivative in appraising the impacts of specific medications and assessing vascular health and aging, offering potential avenues in arteriosclerotic disease screening. Subsequent research has demonstrated the effective application of the second derivative of the PPG waveform in identifying the dicrotic notch within a single pulse wave (see Figure 13), a critical landmark in PWA.

In 2022, Charlton et al. conducted a collaborative study to investigate the hemodynamic characteristics of photoplethysmogram (PPG) waveforms for the purpose of vascular age assessment [64]. A key outcome of their work was the identification of a comprehensive set of features, termed "fiducial points," which could be extracted from the PPG waveform to achieve accurate vascular age estimation.

The term "fiducial" originates from the Latin *fiducialis*, meaning "reliable". In the context of signal processing, it refers to reference points employed for precise measurements. In the early cases, it has been used for accurate determination of pulse transit
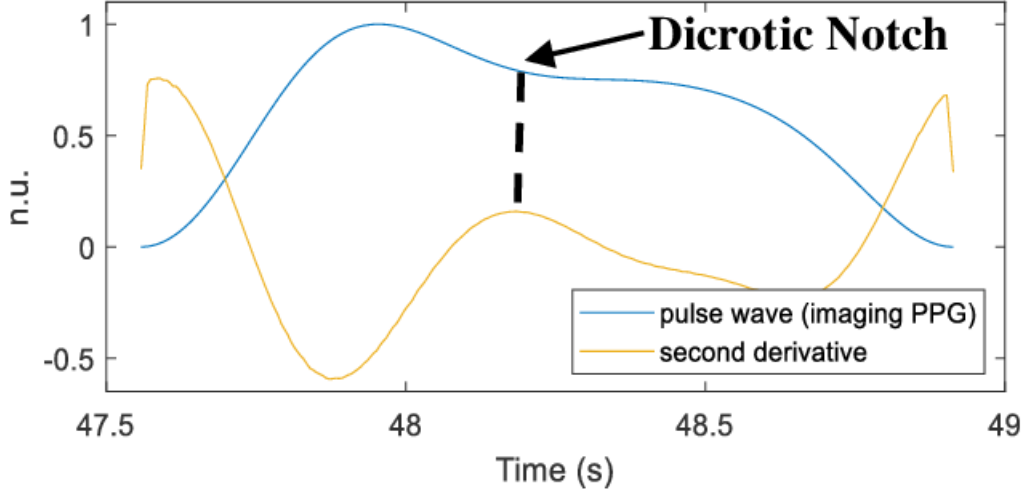
Figure 13: Dicrotic Notch Approximation from the Second Derivate of the PPG [63]

time (PTT) between the R-wave of the electrocardiogram (ECG) and a designated point in a finger PPG pulse, as demonstrated by Zhang et al. [65]. In the study by Charlton et al., these points were repurposed to delineate diverse landmarks (identified as Row A in Figure 14) on the pulse wave, serving as references for extracting both temporal and amplitude-based features.

Building upon the identified fiducial points, Charlton et al. employed various techniques to extract meaningful values from a single PPG signal (Row B in Figure 14) that contribute to vascular age assessment. This section provides a summary of the implemented methods and corresponding example values (presented in brackets):

1. Pulse Wave Features (crest time: time from `onset` to `sys`)

2. First Derivative Features (minimum rise time: amplitude of pulse wave divided by amplitude of `ms`)

3. Second Derivative Features (aging index: defined as amplitude values of `(b-c-d-e)/a`)

4. Combination of Features (minimum rise time: `[1/x0(ms)]·[x(sys) - x(onset)]`)

5. Frequency Domain Analysis (Fast Fourier Transform (FFT) analysis: Use of FFT to extract amplitude and phase information from the PPG signal)

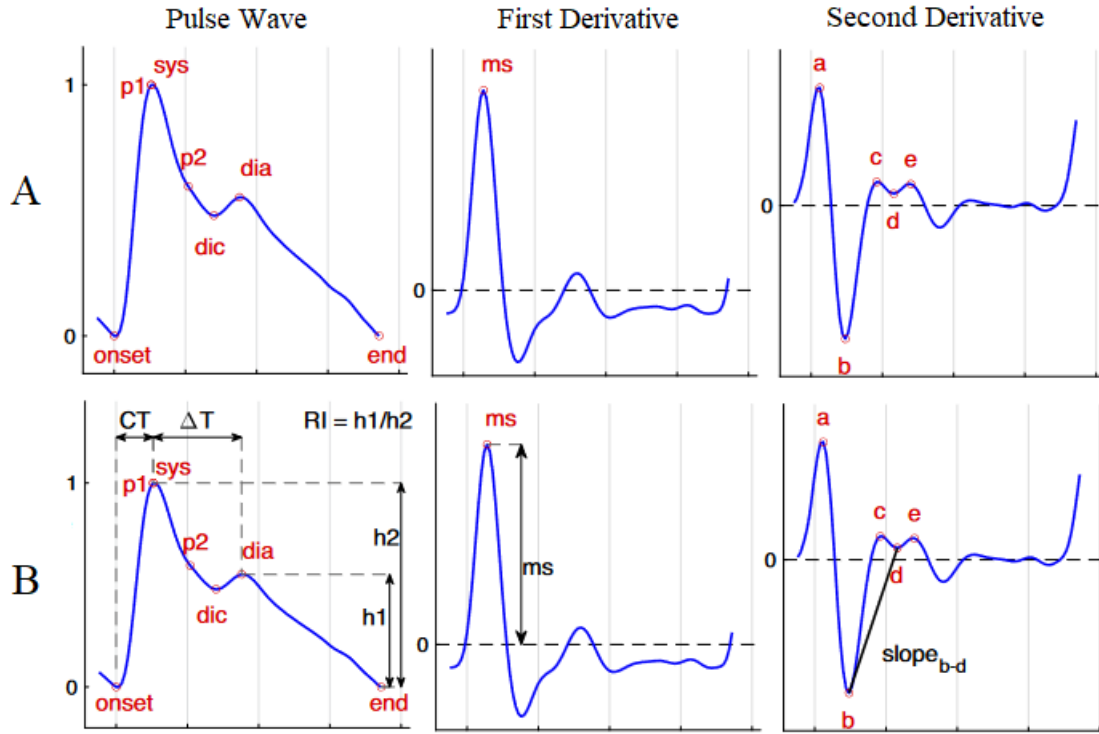6. Features From Multiple Beats (pulse rate variability parameters)

Figure 14: A - Fiducial Point Identification; B - Feature Calculation [64]

This section explored diverse signal processing techniques. As mentioned previously, traditional methods relying on physiological parameters (PAT, PTT, PWV) face limitations. Signal processing approaches like PWA, filtering, and feature extraction are often integrated with ML models and provide a higher BP detection accuracy. These approaches show promising results for cuffless, continuous BP estimation using PPG signals, paving the way for practical non-invasive BP monitoring solutions.

3.2.2 Machine Learning

Building upon the foundation laid by traditional signal processing techniques, ML emerges as a transformative force in the pursuit of accurate and non-invasive BP estimation using PPG signals. This section delves into the diverse tapestry of ML methods currently employed, thoroughly exploring their individual approaches and their collective potential to improve cuffless BP monitoring.

Machine Learning Approaches

BP estimation using ML techniques is data driven, unlike the traditional PTT/PAT only models. Several studies attempted to fit regression models, such as multilinear
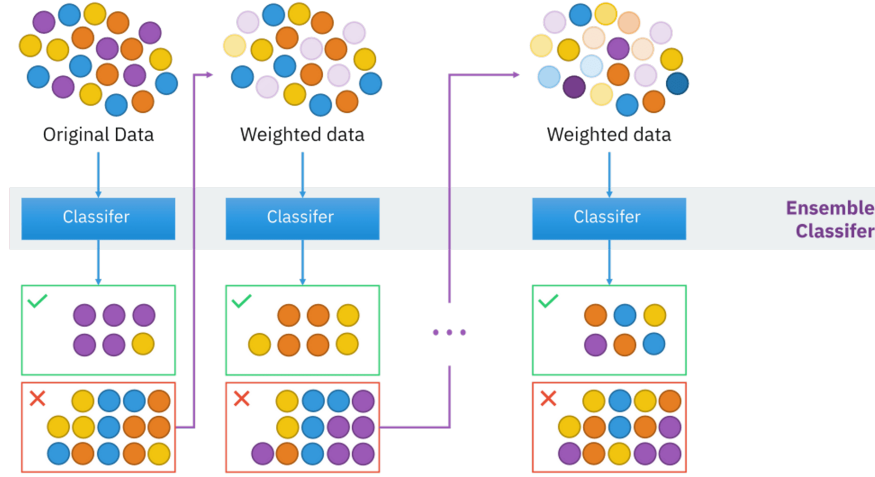
Figure 15: AdaBoost, or Adaptive Boosting, is an ensemble learning technique that iteratively combines weak classifiers to create a strong classifier by adjusting weights based on classification errors [66]

regression, support vector machine (SVM) and random forest, for estimating BP using PTT/PAT based approach with some degree of success, but the results did not always satisfy the international standards.

As early as 2003, Teng and Zhang [67] were among the pioneers in exploring non-invasive methods for estimating blood pressure without the need for traditional cuff-based techniques. They explored the relationship between four PPG features and BP using a linear regression (LR) model. While diastolic time exhibited the strongest correlation with both SBP and DBP, the overall results suggested limitations in LR for accurate BP estimation.

Recognizing these limitations, Suzuki and Oguri (2009) introduced AdaBoost (example in Figure 15), a classifier, for SBP estimation [68]. This methodology segmented SBP values using a threshold before employing a nonlinear ML model, showcasing the need for more complex techniques.

Seeking a different approach, Ruiz-Rodriguez et al. (2013) utilized a Deep Belief Network Restricted Boltzmann Machine (RBM) for simultaneous prediction of SBP, DBP, and MAP [69]. An example DBN and RBM with custom input and output sizes is illustrated in Figure 16 However, the study yielded highly variable results, raising concerns about its reliability.

Shifting focus to feature extraction, Kurylyak et al. (2013) extracted 21 features from the PPG waveform and used a feedforward NN (example in Figure 17) for SBP and
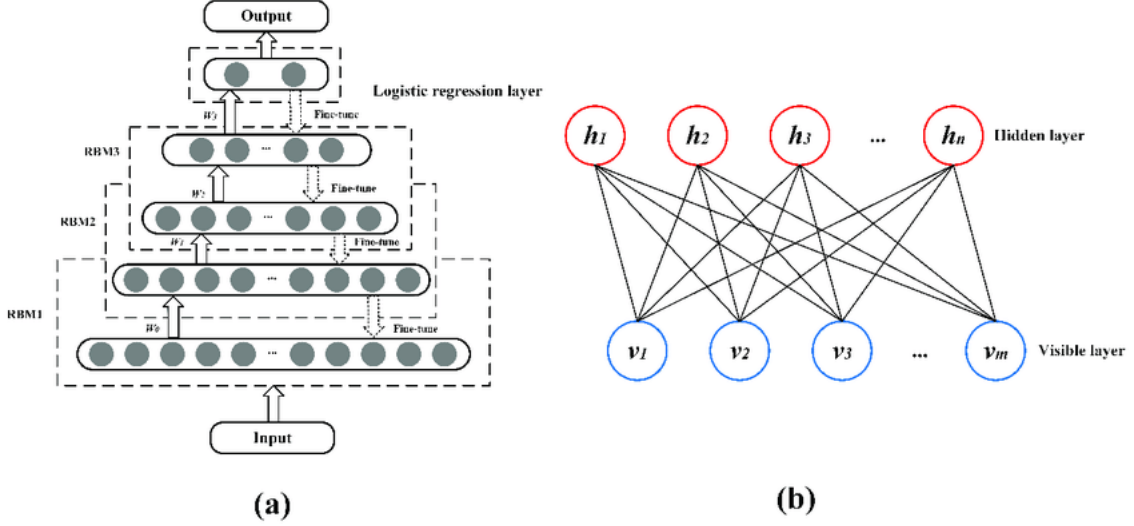
Figure 16: A DBN (a) combines multiple layers of RBMs (b) to form a generative model capable of learning hierarchical representations of the data [70]

DBP estimation [71]. Their promising results demonstrated the potential of NN-based approaches.

Xing and Sun (2016) ventured into the frequency domain, applying Fast Fourier Transformation to select features followed by a feedforward NN for BP estimation [73]. While initial results were encouraging, the authors recognized the need for broader feature space exploration.

Building upon Kurylyak et al.'s work, Liu et al. (2017) incorporated 14 second derivative features and employed an SVM for BP estimation, highlighting the value of diverse feature extraction techniques [74].

Marking a significant shift, Su et al. (2018) explored a four-layer bidirectional Long Short-term memory (LSTM) model with residual connections, demonstrating the promise of recurrent NNs [75]. The working principle of an LSTM is demonstrated in Figure 18.

A 2019 study by Tanveer and Hasan introduced a hierarchical Artificial NN-LSTM model for blood pressure estimation, comprising two levels: the lower level employed ANNs to extract morphological features from ECG and PPG waveforms, while the upper level utilized LSTM layers to address temporal variations in these features [77]. They also found, that DBP is strongly associated with SBP and can enhance its estimation, suggesting simultaneous modeling using a single architecture for both.

Focusing on long term estimation, El-Hajj and Kyriacou (2021) proposed leveraging advanced deep learning techniques like Bidirectional-LSTMs and Bidirectional Gated Recurrent Units (GRU) with attention mechanisms (example of attention mechanism
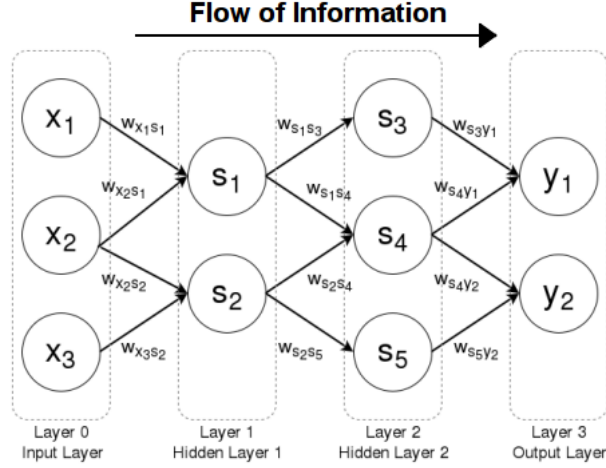
Figure 17: Feed Forward NNs have connections between the nodes that do not form cycles, allowing data to move in only one direction, from the input nodes through the hidden nodes to the output nodes, with each connection having an associated weight [72]

.

implementation in LSTM in Figure 19) for BP estimation [5].

Recognizing the need for real-world applicability, Joung et al. (2023) evaluated a learning-driven cuffless BP estimation system under challenging conditions with calibration [79]. Their 1D convolutional NN highlighted the importance of addressing various real-world scenarios.

These early studies illustrate the evolution of ML techniques for cuffless BP estimation, paving the way for further advancements. From exploring linear relationships to harnessing the power of deep learning, researchers continue to refine and develop novel approaches. While challenges remain, these pioneering efforts demonstrate the immense potential of ML in improving non-invasive BP monitoring, and future research holds the promise for even more accurate and robust solutions.

To conclude, the relationship between PPG characteristics and BP was not found to consistently follow a linear trend. Conventional linear models frequently struggle to effectively capture the complex relationship between BP and PPG when analysed across various demographic datasets. Traditional ML algorithms like SVMs and Random Forest tend to achieve higher accuracy rates in this context. To estimate BP accurately using these techniques, distinct models are typically constructed for SBP and DBP. However, recent evidence suggests that a unified architecture capable of simultaneously modeling SBP, DBP, and even MAP is both feasible and advantageous. Various advanced NN
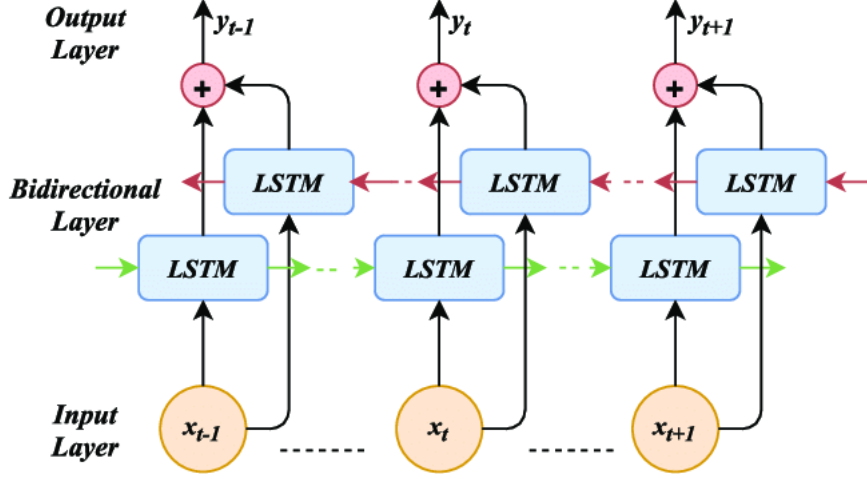
Figure 18: Bidirectional LSTM is a type of recurrent neural network architecture that processes sequential data in both forward and backward directions. This allows the model to capture dependencies from past and future contexts simultaneously, enhancing its ability to understand and predict patterns in sequential data [76]

.

models demonstrate superior efficiency in integrating such architectures and leveraging extensive datasets with heightened precision relative to conventional ML approaches.

4 Methods

The Methods section provides an overview of the methodologies employed in the `PPG-BP` project. It encompasses various sub-directories such as MIMIC and PyTorch tutorials, with the primary code located within the `model` Python Package. Within the `model`, there exist several sub-packages containing relevant data for subsequent project components, while the core code is distributed across five `.py` classes: `init_scripts.py` (Initialization / Data Fetching), `sp_scripts.py` (Signal Processing), `ml_scripts.py` (Machine Learning), `visual.py` (Visualization), and `main.py`, which integrates all the aforementioned components. The whole repository can be found on the author's *GitHub* page [80].

4.1 Data Fetching

The initial phase in virtually all Data Science endeavors involves Data Preparation. This section will examine the `init_scripts.py` class. For this project, data was sourced from the MIMIC-III and MIMIC-IV DBs, each serving distinct purposes. Data from
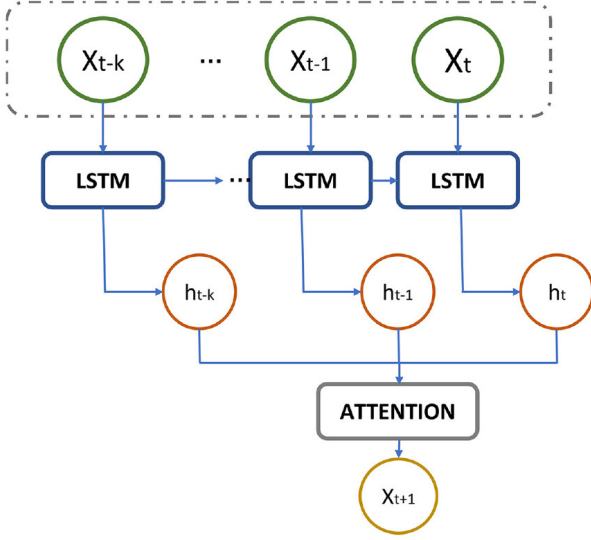
Figure 19: The attention mechanism in LSTM allows the model to focus on specific parts of the input sequence, dynamically adjusting the importance of each input element during the prediction process [78]

the MIMIC-IV DB was employed as the validation dataset (detailed further in the ML methods section 4.3), since it is regarded as the most modern and most reliable MIMIC DB currently available. In contrast, data from the MIMIC-III database was utilized for training and testing ML models due to its significantly larger size. Nevertheless, the data retrieval process employed similar methods for both the older and newer waveform datasets.

Tools and Approaches

Researchers at the MIT Laboratory for Computational Physiology have developed a native Python library named the waveform-database (WFDB) package, facilitating the convenient handling of MIMIC datasets. This library comprises tools for reading, writing, and processing WFDB signals and annotations [81]. Efficient and consistent data retrieval was achieved through a combination of pre-existing WFDB library functions and custom-written methods.

First of all, a list of all of the records from the selected DB were fetched utilizing the

```
wfdb.get_record_list(db_name)
```

method. Then an iterative process followed, going through all of the subjects from the loaded records list. When assessing a single subject, the same method, but with more specific parameters

```
wfdb.get_record_list((f'db_name/subject')
```

was called, in this instance to load all studies from a single subject. Another loop was formed to iterate through each study within the subject. These studies consist of records,

each representing a single ICU "session", during which the patient was connected to at least one monitoring device, therefore they highly differ in time length. Given the diversity of monitoring devices, these records encompass various signals, including ECG, ABP, and Pleth (equivalent to PPG). To verify if the record includes all the required signals (ABP and Pleth for this study), the method

```
record_data = wfdb.rdheader(subject.name, record_dir, rd_segments=True)
```

was invoked, providing the header data of a single record, which is then used to fetch all present signals

```
signal_names = record_data.sig_name.
```

If the record lacks either the *ABP* or *Pleth* signals, it is excluded from further processing. However, even a single record comprises multiple segments, varying in duration and the signals they capture. If a record lacks either the ABP or Pleth signals, it is excluded from further processing. Each record comprises multiple segments, varying in duration and the signals they capture. In addition to signal requirements, segments must also have a minimum length of 10 minutes to be considered usable. This criterion aims to ensure data reliability and variability, as longer segments offer more data points to represent physiological states accurately, reducing the impact of short-term fluctuations and noise. The segment duration length is determined by the following function:

```
segment_metadata = wfdb.rdheader(segment, record_dir)
tot_seg_length = segment_metadata.sig_len
sampling_rate = segment_metadata.fs
seg_duration = tot_seg_length / fs
```

Precisely these segments represent the smallest data samples utilized in this study, containing continuous numeric values sampled at a specific frequency rate. The data abstraction levels in MIMIC DBs can be depicted by the chart, showing a descending order from left to right:

$$Subject \rightarrow Study \rightarrow Record \rightarrow Segment$$

An iterative process is likewise applied to every segment of a record, by fetching all values from a single segment:

```
segment_data = wfdb.rdrecord(segment, record_dir).
```

These segments should also be devoid of any "faulty" values, identified as NumPy values `NaN` and `inf`. For ABP segments values outside the range of 30 to 250 (accounting for extreme and likely erroneous measurements) are omitted, and for Pleth values must strictly fall between 0 and 1 (representing the valid PPG range). These exclusion criteria

are summarized in Table 1.

If a 10-minute part of the segment matches these criteria, it is saved to the `./mimic3` (or `./mimic4`) directory, as 2 separate and synchronous ABP and PPG files. If a segment is longer than 10 minutes, then more 10 minute segments may be extracted (marked by a _ and a number representing the *n-th* 10 minute part of a segment) Examples of the file names and their values are illustrated in Figures **??**.

As noted earlier, each subject in the database may encompass multiple studies, records, and segments. To prevent disproportionate representation of individual patient data, a limit of 100 segments, each spanning 10 minutes, was imposed per subject. This is specifically important for data retrieval from the MIMIC-III database, which is intended for training and testing purposes. However, this restriction was not applied to data retrieval from the MIMIC-IV database, which is designated for validation purposes and aims to encompass all available 10-minute segments, thus simulating real-world data where over-representation is not a concern.

Additionally, the primary objective was to achieve a dataset split ratio of 60/20/20 for training, testing, and validation, where 80% of the data comprises the MIMIC-III dataset for training and testing (60/20), and the remaining 20% consists of the MIMIC-IV dataset for validation purposes. To facilitate this, an initial set of x segments was retrieved from the MIMIC-IV database, followed by obtaining four times the number of x segments from the MIMIC-III database. However, it is important to acknowledge that the quantity of segments obtained from each database doesn't directly correspond to the number of features utilized in the ML phase, as signal processing (SP) tasks are performed in between. Thus, the 60/20/20 split ratio for training, testing, and validation serves more as a guideline than an absolute target for the number of segments retrieved. Details on

ABP	Pleth
30 < x < 250	0 < x < 1
not NaN, inf	

Table 1: Criteria for non-faulty values in data fetching

abp_80057524_0005_0

ppg_89746514_0020_18

signal record segment
n-th 10min segment part

Figure 20: Examples of extracted segment files

Figure 21: Example raw ABP and PPG values

achieving the actual proportions are provided in the subsequent section 4.2.

4.2 Signal Processing

4.2.1 Filtering Aproaches

butter + savgol optimal, because PPG shapes best (show pic)

4.2.2 Beat Finding Algorithms

3 beat findings algos from wfdb methods, 1 novel for reference
  Beat grouping and synchronization
  Mention that no manual selection was done, due to large size of samples

4.2.3 Fiducial Point detection

wfdb default algos
  cave for dic notch

4.2.4 Feature Extraction

graphics for all 34 features
  explain each significance
  FFT formula

4.3 Machine Learning

LR, MLP, LSTM, GRU models tried
  elaborate splitting approach

1. Digital signal filtering using Savitzky-Golay and Butterworth Lowpass filters.

2. Beat detection algorithms from MIMIC WFDB Tutorial used for primary estimation. Beat detection improved with manual implementation of SciPy library.

3. Fiducial Point calculation based on the algorithm provided in the MIMIC WFDB Tutorial.

4. Feature extraction with personally created code to extract time domain features, and NumPy library to extract frequency domain features (FFT). Median value calculation using NumPy library.

31

5. Machine Learning Model creation using PyTorch and Scikit-Learn libraries.

5 Results

5.1 Data Fetching

Data for Validation from MIMIC4: 5508 records each containing 37795 values corresponding to 605 seconds (fs=64.4725);

Data for Training/Testing from MIMIC3 (1st Iteration): 22083 (4*MIMIC4) records each containing 75625 values corresponding to 605 seconds (fs=125);

5.2 Data Processing

Same Signaling processing approaches were included (see 4.2) for both the MIMIC4 and MIMIC3 data.

5.3 Feature Extraction

CAVE: out of the 34 features, 2 (delta T and resistive index) depend on the accurate detection of the dicrotic notch. Significantly more values can be extracted if finding the dicrotic notch would not be necessary

FE from MIMIC4 for Validation: - For target reference Systolic, Diastolic and MAP values were extracted from the waveform data. - For Machine Learning, 34 features were extracted from the PPG waveform A total of **1,309,265** values were extracted, resulting in a 34 x 1,309,265 matrix. Total of **183,140** median values were extracted.

FE from MIMIC3 for Training/Testing:

- For target reference ABP Systolic, Diastolic and MAP values were extracted from the waveform data. - For Machine Learning, 34 features were extracted from the PPG waveform A total of **13,659,375** values were extracted, resulting in a 34 x 13659375 matrix. Total of **1,918,623** median values were extracted.

The summarized results are displayed in Figure 22.
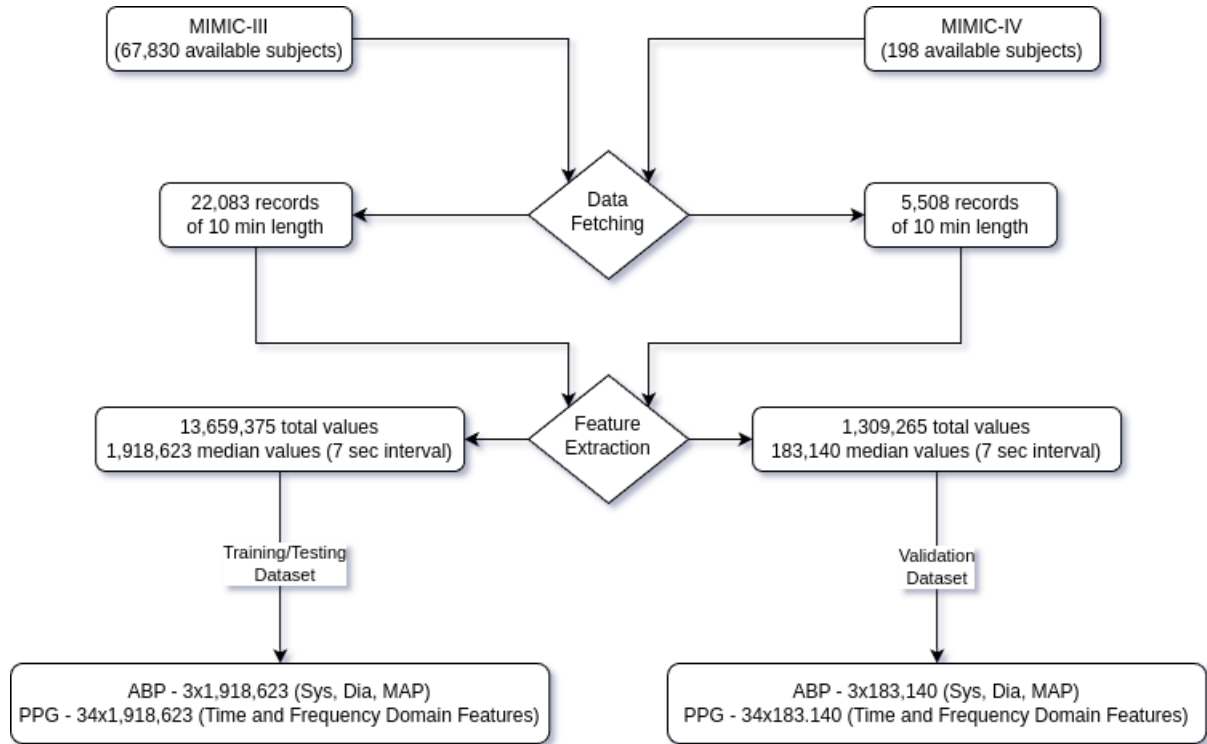
Figure 22: Flow Diagram presenting the Data Fetching and Processing

5.4 Machine Learning

6 Discussion

Limitations: - not knowing what devices were used - how they were calibrated - how accurate they are - pulse oximeter and arterial catheter parameters - sampling rates are different for every device (even between MIMIC 3 and 4)

Possible Improvements: - integrate both the ECG and PPG graphs for a more precise prediction - use further signal processing approaches - manually filter waveform graphics (e.g. faulty PPG signal) - expand on machine learning algorithms - experiment with different median intervals

7 Conclusion

References

[1] W. H. Organization, *World Health Statistics 2023: Monitoring Health for the SDGs, Sustainable Development Goals.* World Health Organization.

[2] M. Ezzati, A. D. Lopez, A. Rodgers, S. Vander Hoorn, and C. J. Murray, "Selected major risk factors and global and regional burden of disease," vol. 360, no. 9343, pp. 1347–1360.

[3] V. Burt, P. Whelton, E. Roccella, C. Brown, J. Cutler, M. Higgins, M. Horan, and D. Labarthe, "Prevalence of hypertension in the US adult population: Results from the third National Health and Nutrition Examination Survey, 1988-1991," vol. 25, no. 3, pp. 305–313.

[4] C. Poon and Y. Zhang, "Cuff-less and Noninvasive Measurements of Arterial Blood Pressure by Pulse Transit Time," in *2005 IEEE Engineering in Medicine and Biology 27th Annual Conference*, pp. 5877–5880.

[5] C. El-Hajj and g.-i. family=Kyriacou, given=PA, "Deep learning models for cuffless blood pressure monitoring from PPG signals using attention mechanism," vol. 65, p. 102301.

[6] M. Sharma, K. Barbosa, V. Ho, D. Griggs, T. Ghirmai, S. K. Krishnan, T. K. Hsiai, J.-C. Chiao, and H. Cao, "Cuff-Less and Continuous Blood Pressure Monitoring: A Methodological Review," vol. 5, no. 2, p. 21.

[7] A. A. Leung, K. Nerenberg, S. S. Daskalopoulou, K. McBrien, K. B. Zarnke, K. Dasgupta, L. Cloutier, M. Gelfer, M. Lamarre-Cliche, A. Milot, P. Bolli, G. Tremblay, D. McLean, S. W. Tobe, M. Ruzicka, K. D. Burns, M. Vallée, G. V. R. Prasad, M. Lebel, R. D. Feldman, P. Selby, A. Pipe, E. L. Schiffrin, P. A. McFarlane, P. Oh, R. A. Hegele, M. Khara, T. W. Wilson, S. B. Penner, E. Burgess, R. J. Herman, S. L. Bacon, S. W. Rabkin, R. E. Gilbert, T. S. Campbell, S. Grover, G. Honos, P. Lindsay, M. D. Hill, S. B. Coutts, G. Gubitz, N. R. C. Campbell, G. W. Moe, J. G. Howlett, J.-M. Boulanger, A. Prebtani, P. Larochelle, L. A. Leiter, C. Jones, R. I. Ogilvie, V. Woo, J. Kaczorowski, L. Trudeau, R. J. Petrella, S. Hiremath, D. Drouin, K. L. Lavoie, P. Hamet, G. Fodor, J. C. Grégoire, R. Lewanczuk, G. K. Dresser, M. Sharma, D. Reid, S. A. Lear, G. Moullec, M. Gupta, L. A. Magee, A. G. Logan, K. C. Harris, J. Dionne, A. Fournier, G. Benoit, J. Feber, L. Poirier, R. S.

Padwal, D. M. Rabi, and CHEP Guidelines Task Force, "Hypertension Canada's 2016 Canadian Hypertension Education Program Guidelines for Blood Pressure Measurement, Diagnosis, Assessment of Risk, Prevention, and Treatment of Hypertension," vol. 32, no. 5, pp. 569–588.

[8] P. Sebo, A. Pechère-Bertschi, F. R. Herrmann, D. M. Haller, and P. Bovier, "Blood pressure measurements are unreliable to diagnose hypertension in primary care," vol. 32, no. 3, pp. 509–517.

[9] I. Reyes, H. Nazeran, M. Franco, and E. Haltiwanger, "Wireless photoplethysmographic device for heart rate variability signal acquisition and analysis," in *2012 Annual International Conference of the IEEE Engineering in Medicine and Biology Society*, pp. 2092–2095.

[10] G. Yoon, J. Y. Lee, K. J. Jeon, K.-K. Park, H. S. Yeo, H. T. Hwang, H. S. Kim, and I.-D. Hwang, "Multiple diagnosis based on photoplethysmography: Hematocrit, SpO2, pulse, and respiration," in *Optics in Health Care and Biomedical Optics: Diagnostics and Treatment*, vol. 4916, pp. 185–188, SPIE.

[11] S. Knight, J. Lipoth, M. Namvari, C. Gu, M. Hedayati Ch, S. Syed-Abdul, and R. J. Spiteri, "The Accuracy of Wearable Photoplethysmography Sensors for Telehealth Monitoring: A Scoping Review,"

[12] "What is blood pressure and how is it measured?," in *InformedHealth.Org [Internet]*, Institute for Quality and Efficiency in Health Care (IQWiG).

[13] J. G. Betts, K. A. Young, J. A. Wise, E. Johnson, B. Poe, D. H. Kruse, O. Korol, J. E. Johnson, M. Womble, P. DeSaix, J. G. Betts, K. A. Young, J. A. Wise, E. Johnson, B. Poe, D. H. Kruse, O. Korol, J. E. Johnson, M. Womble, and P. DeSaix, "20.2 Blood Flow, Blood Pressure, and Resistance - Anatomy and Physiology 2e — OpenStax."

[14] A. J. Naylor, D. I. Sessler, K. Maheshwari, A. K. Khanna, D. Yang, E. J. Mascha, I. Suleiman, E. M. Reville, D. Cote, M. T. Hutcherson, B. M. Nguyen, H. Elsharkawy, and A. Kurz, "Arterial Catheters for Early Detection and Treatment of Hypotension During Major Noncardiac Surgery: A Randomized Trial," vol. 131, no. 5, pp. 1540–1550.

[15] D. Ettehad, C. A. Emdin, A. Kiran, S. G. Anderson, T. Callender, J. Emberson, J. Chalmers, A. Rodgers, and K. Rahimi, "Blood pressure lowering for prevention of cardiovascular disease and death: A systematic review and meta-analysis," vol. 387, no. 10022, pp. 957–967.

[16] "Standard Sphygmomanometer."

[17] "Automatic Digital Blood Pressure Monitor."

[18] V. L. Clark and J. A. Kruse, "Arterial catheterization," vol. 8, no. 4, pp. 687–697.

[19] B. L. Hill, N. Rakocz, Rudas, J. N. Chiang, S. Wang, I. Hofer, M. Cannesson, and E. Halperin, "Imputation of the continuous arterial line blood pressure waveform from non-invasive measurements using deep learning," vol. 11, p. 15755.

[20] N. T. Contributor, "Essential critical care skills 3: Arterial line care."

[21] L.-w. H. Lehman, M. Saeed, D. Talmor, R. Mark, and A. Malhotra, "Methods of Blood Pressure Measurement in the ICU," vol. 41, no. 1, pp. 34–40.

[22] D. DeMers and D. Wachs, "Physiology, Mean Arterial Pressure," in *StatPearls*, StatPearls Publishing.

[23] C.-S. Kim, A. M. Carek, O. T. Inan, R. Mukkamala, and J.-O. Hahn, "Ballistocardiogram-Based Approach to Cuffless Blood Pressure Monitoring: Proof of Concept and Potential Challenges," vol. 65, no. 11, pp. 2384–2391.

[24] B. Imholz, W. Wieling, G. Van Montfrans, and K. Wesseling, "Fifteen years experience with finger arterial pressure monitoring: Assessment of the technology," vol. 38, no. 3, pp. 605–616.

[25] L. Peter, N. Noury, and M. Cerny, "A review of methods for non-invasive and continuous blood pressure monitoring: Pulse transit time method is promising?," vol. 35, no. 5, pp. 271–282.

[26] A. V. J. Challoner and C. A. Ramsay, "A photoelectric plethysmograph for the measurement of cutaneous blood flow," vol. 19, no. 3, p. 317.

[27] H. Molitor and M. Kniazuk, "A New Bloodless Method for Continuous Recording of Peripheral Circulatory Changes," vol. 57, no. 1, pp. 6–18.

[28] A. B. Hertzman, "Photoelectric Plethysmography of the Fingers and Toes in Man," vol. 37, no. 3, pp. 529–534.

[29] S. Srivastav, R. T. Jamil, and R. Zeltser, "Valsalva Maneuver," in *StatPearls*, StatPearls Publishing.

[30] I. Yoshiya, Y. Shimada, and K. Tanaka, "Spectrophotometric monitoring of arterial oxygen saturation in the fingertip," vol. 18, no. 1, pp. 27–32.

[31] T. Aoyagi and K. Miyasaka, "Pulse oximetry: Its invention, contribution to medicine, and future tasks," vol. 94, pp. S1–3.

[32] F. P. Wieringa, F. Mastik, and A. F. W. van der Steen, "Contactless multiple wavelength photoplethysmographic imaging: A first step toward "SpO2 camera" technology," vol. 33, no. 8, pp. 1034–1041.

[33] S. Rhee, B.-H. Yang, and H. Asada, "Artifact-resistant power-efficient design of finger-ring plethysmographic sensors," vol. 48, no. 7, pp. 795–805.

[34] D. Zheng and Y. Zhang, "A ring-type device for the noninvasive measurement of arterial blood pressure," in *Proceedings of the 25th Annual International Conference of the IEEE Engineering in Medicine and Biology Society (IEEE Cat. No.03CH37439)*, vol. 4, pp. 3184–3187 Vol.4.

[35] H. Lee, H. Ko, and J. Lee, "Reflectance pulse oximetry: Practical issues and limitations," vol. 2, no. 4, pp. 195–198.

[36] P. Mohan, N. Velmurugan, and J. Vignesh, "Spot measurement of heart rate based on morphology of PhotoPlethysmoGraphic (PPG) signals," vol. 41, pp. 1–10.

[37] J. Allen, "Photoplethysmography and its application in clinical physiological measurement," vol. 28, no. 3, p. R1.

[38] A. M. Weissler, W. S. Harris, and C. D. Schoenfeld, "Systolic time intervals in heart failure in man," vol. 37, no. 2, pp. 149–159.

[39] N. Sviridova and K. Sakai, "Human photoplethysmogram: New insight into chaotic characteristics," vol. 77, pp. 53–63.

[40] D. Castaneda, A. Esparza, M. Ghamari, C. Soltanpur, and H. Nazeran, "A review on wearable photoplethysmography sensors and their potential future applications in health care," vol. 4, no. 4, pp. 195–202.

[41] A. Ponnada, "Technological considerations for sensor-assisted chronic pain assessment in natural environments."

[42] S. Zanelli, M. El Yacoubi, M. Hallab, and M. Ammi, "On the potential of AI based health assessment from photopletysmographic signals,"

[43] G. Langewouters, A. Zwart, R. Busse, and K. Wesseling, "Pressure-diameter relationships of segments of human finger arteries," vol. 7, no. 1, pp. 43–55.

[44] G. Moody and R. Mark, "A database to support development and evaluation of intelligent intensive care monitoring," in *Computers in Cardiology 1996*, pp. 657–660.

[45] M. Saeed, M. Villarroel, A. T. Reisner, G. Clifford, L.-W. Lehman, G. Moody, T. Heldt, T. H. Kyaw, B. Moody, and R. G. Mark, "Multiparameter Intelligent Monitoring in Intensive Care II (MIMIC-II): A public-access intensive care unit database," vol. 39, no. 5, pp. 952–960.

[46] A. E. W. Johnson, T. J. Pollard, L. Shen, L.-w. H. Lehman, M. Feng, M. Ghassemi, B. Moody, P. Szolovits, L. Anthony Celi, and R. G. Mark, "MIMIC-III, a freely accessible critical care database," vol. 3, no. 1, p. 160035.

[47] A. E. W. Johnson, L. Bulgarelli, L. Shen, A. Gayles, A. Shammout, S. Horng, T. J. Pollard, S. Hao, B. Moody, B. Gow, L.-w. H. Lehman, L. A. Celi, and R. G. Mark, "MIMIC-IV, a freely accessible electronic health record dataset," vol. 10, no. 1, p. 1.

[48] P. H. Charlton, "MIMIC WFDB Tutorials."

[49] B. Moody, G. Moody, M. Villarroel, G. Clifford, and I. Silva, "MIMIC-III Waveform Database."

[50] B. Moody, S. Hao, B. Gow, T. Pollard, W. Zong, and R. Mark, "MIMIC-IV Waveform Database."

[51] R. Mukkamala, J.-O. Hahn, O. T. Inan, L. K. Mestha, C.-S. Kim, H. Töreyin, and S. Kyal, "Toward Ubiquitous Blood Pressure Monitoring via Pulse Transit Time: Theory and Practice," vol. 62, no. 8, pp. 1879–1901.

[52] H. W. Lui and K. Chow, "A Novel Calibration Procedure of Pulse Transit Time based Blood Pressure measurement with Heart Rate and Respiratory Rate," vol. 2018.

[53] M. S. Dhillon and M. J. Banet, "Pulse Arrival Time Techniques," in *The Handbook of Cuffless Blood Pressure Monitoring: A Practical Guide for Clinicians, Researchers, and Engineers* (J. Solà and R. Delgado-Gonzalo, eds.), pp. 43–59, Springer International Publishing.

[54] D. B. McCombie, A. T. Reisner, and H. H. Asada, "Adaptive blood pressure estimation from wearable PPG sensors using peripheral artery pulse wave velocity measurements and multi-channel blind identification of local arterial dynamics," vol. 2006, pp. 3521–3524.

[55] M. Urban, "Understanding Arterial Biomechanics with Ultrasound and Waveguide Models," vol. 19, p. 46.

[56] M. Elgendi, "On the Analysis of Fingertip Photoplethysmogram Signals," vol. 8, no. 1, pp. 14–25.

[57] V. Bikia, T. Fong, R. Climie, R. Bruno, B. Hametner, C. Mayer, D. Terentes-Printzios, and P. Charlton, "Leveraging the potential of machine learning for assessing vascular ageing: State-of-the-art and future research," vol. 2.

[58] A. Chatterjee and U. K. Roy, "PPG Based Heart Rate Algorithm Improvement with Butterworth IIR Filter and Savitzky-Golay FIR Filter," in *2018 2nd International Conference on Electronics, Materials Engineering & Nano-Technology (IEMENTech)*, pp. 1–6.

[59] g.-i. family=Savitzky, given=Abraham. and M. J. E. Golay, "Smoothing and Differentiation of Data by Simplified Least Squares Procedures.," vol. 36, no. 8, pp. 1627–1639.

[60] A. Antoniou, *Digital Filters: Analysis, Design, and Signal Processing Applications.* McGraw-Hill Education, 1st edition ed.

[61] Y. Liang, M. Elgendi, Z. Chen, and R. Ward, "An optimal filter for short photoplethysmogram signals," vol. 5, no. 1, p. 180076.

[62] K. Takazawa, N. Tanaka, M. Fujita, O. Matsuoka, T. Saiki, M. Aikawa, S. Tamura, and C. Ibukiyama, "Assessment of vasoactive agents and vascular aging by the second derivative of photoplethysmogram waveform," vol. 32, no. 2, pp. 365–370.

[63] D. Djeldjli, F. Bousefsaf, C. Maaoui, and F. Reguig, "Imaging Photoplethysmography: Signal Waveform Analysis," pp. 830–834.

[64] P. H. Charlton, B. Paliakaitė, K. Pilt, M. Bachler, S. Zanelli, D. Kulin, J. Allen, M. Hallab, E. Bianchini, C. C. Mayer, D. Terentes-Printzios, V. Dittrich, B. Hametner, D. Veerasingam, D. Žikić, and V. Marozas, "Assessing hemodynamics from the photoplethysmogram to gain insights into vascular age: A review from VascAgeNet," vol. 322, no. 4, pp. H493–H522.

[65] X.-Y. Zhang and Y.-T. Zhang, "The effect of local cold exposure on pulse transit time," vol. 2005, pp. 3522–3525.

[66] "AdaBoost Algorithm in Machine Learning."

[67] X. Teng and Y. Zhang, "Continuous and noninvasive estimation of arterial blood pressure using a photoplethysmographic approach," in *Proceedings of the 25th Annual International Conference of the IEEE Engineering in Medicine and Biology Society (IEEE Cat. No.03CH37439)*, vol. 4, pp. 3153–3156 Vol.4.

[68] S. Suzuki and K. Oguri, "Cuffless blood pressure estimation by error-correcting output coding method based on an aggregation of AdaBoost with a photoplethysmograph sensor," in *2009 Annual International Conference of the IEEE Engineering in Medicine and Biology Society*, pp. 6765–6768.

[69] J. C. Ruiz-Rodríguez, A. Ruiz-Sanmartín, V. Ribas, and J. Caballero, "Innovative continuous non-invasive cuffless blood pressure monitoring based on photoplethysmography technology," vol. 39, no. 9, pp. 1618–1625.

[70] C. Ou, J. Yang, Z. Du, X. Zhang, and D. Zhu, "Integrating Cellular Automata with Unsupervised Deep-Learning Algorithms: A Case Study of Urban-Sprawl Simulation in the Jingjintang Urban Agglomeration, China," vol. 11.

[71] Y. Kurylyak, F. Lamonaca, and D. Grimaldi, "A Neural Network-based method for continuous blood pressure estimation from a PPG signal," in *2013 IEEE International Instrumentation and Measurement Technology Conference (I2MTC)*, pp. 280–283.

[72] "Feedforward Neural Networks — Brilliant Math & Science Wiki."

[73] X. Xing and M. Sun, "Optical blood pressure estimation with photoplethysmography and fft-based neural networks," vol. 7, no. 8, pp. 3007–3020.

[74] M. Liu, X. Zhan, J. Tu, B. Liu, and Z. Zhu, "Integrated navigation for tethered nano-satellite system by modified input-delay neural networks and PROSAC," vol. 2017-May, pp. 202–210.

[75] P. Su, X.-R. Ding, Y.-T. Zhang, J. Liu, F. Miao, and N. Zhao, "Long-term blood pressure prediction with deep recurrent neural networks," in *2018 IEEE EMBS International Conference on Biomedical & Health Informatics (BHI)*, pp. 323–328.

[76] Anishnama, "Understanding Bidirectional LSTM for Sequential Data Processing."

[77] M. S. Tanveer and M. K. Hasan, "Cuffless blood pressure estimation from electrocardiogram and photoplethysmogram using waveform based ANN-LSTM network," vol. 51, pp. 382–392.

[78] G. Marulanda, J. Cifuentes, A. Bello, and J. Reneses, "A hybrid model based on LSTM neural networks with attention mechanism for short-term wind power forecasting," p. 0309524X231191163.

[79] J. Joung, C.-W. Jung, H.-C. Lee, M.-J. Chae, H.-S. Kim, J. Park, W.-Y. Shin, C. Kim, M. Lee, and C. Choi, "Continuous cuffless blood pressure monitoring using photoplethysmography-based PPG2BP-net for high intrasubject blood pressure variations," vol. 13, p. 8605.

[80] H. Jasinskas, "Htjas/PPG-BP."

[81] "MIT-LCP/wfdb-python."